Unfolding of the Tetrameric Loop Deletion Mutant of ROP Protein Is a Second-Order Reaction†

Michael W. Lassalle and Hans-Jürgen Hinz*

Institut für Physikalische Chemie der Westfälischen Wilhelms-Universität, Schlossplatz 4/7, 48161 Münster, Germany

Received December 12, 1997; Revised Manuscript Received March 31, 1998

ABSTRACT: Comprehensive kinetic studies were carried out on the unfolding properties of RM6 as a function of GdnHCl concentration and temperature. This protein is a mutant resulting from the dimeric wild-type CoLE1-ROP protein by deletion of 5 amino acids (Asp 30, Ala 31, Asp 32, Glu 33, Gln 34) in the loop of each monomer. The deletion has dramatic consequences. The dimeric 4-α-helix structure characteristic of the wild-type protein is completely reorganized and the RM6 structure can be described as a tetrameric α helix of extended monomers without loops. These extraordinary structural changes are accompanied by an enormous increase in transition temperature from 71 to 101 °C. These features have been discussed in a separate publication (*1*). The remarkable change in thermal stability of RM6 should be reflected in significant changes in the folding rate constants. This was observed in the present unfolding studies. Decay of tetrameric RM6 was monitored by circular dichroism (CD) and fluorescence to probe for changes in both secondary and tertiary structure, respectively. The identity of the kinetic parameters obtained from the two techniques supports the view that secondary and tertiary structure break down simultaneously. However, the most intriguing result is the finding that unfolding of tetrameric RM6 can be described very well by a second-order reaction. The magnitude of the second-order rate constant k_2 varies dramatically with both temperature and denaturant concentration. At 25 °C and 6.5 M GdnHCl concentration k_2 is 4200 L·(mol of dimer)$^{-1}$·s^{-1}, whereas at 4.4 M GdnHCl a value of $k_2 = 0.9$ L·(mol of dimer)$^{-1}$·s^{-1} is observed. Correspondingly, apparent activation enthalpies show a strong increase from $\Delta H^{\#} = 29.1$ kJ·mol^{-1} at 6.5 M GdnHCl to $\Delta H^{\#} = 79.7$ kJ·mol^{-1} at 4.4 M GdnHCl. A mechanism involving a dimeric intermediate is suggested which permits a consistent interpretation of the findings.

The mechanism of folding of proteins is still far from being understood despite the multitude of careful studies on a broad variety of different proteins (*2*−*9*). Much emphasis has been placed in recent years with impressive results on the elucidation of the in vivo folding of nascent polypeptide chains. It has been established that in vivo folding is often kinetically optimized by involving helper proteins that appear to reduce drastically the number of and the residence time in incorrectly folded structures (*10*−*13*). In view of these exciting results, the interpretation of the spontaneous, unchaperoned folding mechanism in terms of physical principles appears to attract momentarily less attention. However, this is certainly not justified, since spontaneous in vitro folding is far from being understood, as the most recent new hypotheses of the folding mechanism demonstrate (*14*−*16*).

Furthermore spontaneous folding remains the fundamental paradigm independent of whether the process is additionally controlled by helper proteins in vivo. In the present study we provide evidence for the fact that slight digressions from the standard research object of very small monomeric proteins lead to rather unexpected results. This has been exemplified by kinetic studies on the unfolding of the unusual tetrameric 4-α-helix protein, RM6, which is formed from the dimeric wild-type ROP protein by deletion of the five amino acids **(**Asp 30, Ala 31, Asp 32, Glu 33, Gln 34) in the loop region.

The intriguing result of these studies is the fact that RM6 follows strictly a second-order unfolding reaction. This finding is highly unusual, since all unfolding processes studied so far could be described as first-order processes.

ROP protein has been established as a significant model system for the analysis of folding characteristics of dimeric coiled-coil structures (*17*−*21*) together with similar proteins such as human growth hormone-receptor, arc repressor, GCN4 leucine zipper peptide, and TRP repressor (*22*−*27*). RM6 is a particularly interesting system for kinetic investigations due to its tetrameric structure and its extremely high stability which is manifest in an unfolding temperature of $T_{1/2} = 101$ °C at a protein concentration of 1 mg·mL^{-1} (153.3 μM of monomer), a transition enthalpy of $\Delta H_{cal} = 1073 \pm 30$ kJ·(mol of tetramer)$^{-1}$, and a standard Gibbs energy of unfolding of $\Delta G^{\circ}_{D} = 195.1 \pm 5$ kJ·(mol of tetramer)$^{-1}$ at $T = 25$ °C (*1*). Another outstanding feature of RM6 is its extremely slow unfolding kinetics. This can lead to the observation of hysteresis phenomena in the GdnHCl induced unfolding curves, unless provision is taken in establishing equilibrium.

† This research was supported by a scholarship from the Stiftung Stipendien-Fonds des Verbandes der Chemischen Industrie e.V. to M.W.L. and by grants from the European Community Bridge program and the DFG to H.-J.H.

* To whom correspondence should be addressed. Fax: 0049 251 832 9163. E-mail: hinz@nwz.uni-muenster.de.

S0006-2960(97)03069-9 CCC: $15.00
Published on Web 05/19/1998

MATERIALS AND METHODS

Materials

The experiments were performed in 10 mM sodium phosphate, 10 mM Na_2SO_4, and 1 mM EDTA at pH 7. All chemicals used were of reagent grade. The buffer solutions were prepared using quartz-bidistilled water. Before use in equilibrium dialysis, they were routinely filtered, employing Millipore membrane filters of pore size 0.22 μm. Concentrations of GdnHCl were determined by refractive index measurements using the values tabulated by Nozaki (*28*). In the long-term kinetic measurements the GdnHCl concentration was controlled daily.

Methods

Cell Preparation and Protein Purification. Construction of the RM6 gene was performed by G. Cesareni and has been described in Castagnoli et al. (*29*). Cell preparation and purification were identical to those of other mutants of ROP and have been described in Steif et al. (*17*).

Determination of Protein Concentration. For the determination of the protein concentration, a double-beam UV/vis spectrophotometer 554 (model Lambda 5) from Perkin-Elmer or a diode array-x-dap spectrophotometer from IKS Optoelektronik was used. The UV spectra reported have been measured in the wavelength range 240−380 nm using a 1 cm cuvette. The concentration was determined at 280 nm using an absorption coefficient of 0.25 $mL \cdot mg^{-1} \cdot cm^{-1}$ for a 1 mg/mL solution and a light path of 1 cm. The absorption coefficient was calculated according to Perkins (*30*). The molar mass used for the calculation of concentrations in terms of tetramers is $M = 26\,084$ $g \cdot mol^{-1}$.

Fluorescence Measurements. Fluorescence measurements of unfolding of RM6 were performed using a Spex Fluoromax fluorimeter thermostated by a Haake water bath (Haake F3). Thirty-two sample vials were prepared containing GdnHCl concentrations from 0 to 6.5 M increasing at intervals of about 0.2 M. Protein stock solution (4.5 mg/mL) was injected into each vial to a final protein concentration of 0.04 mg/mL (3 μM of dimer). Every 24 h the fluorescence of all 32 samples was determined. To avoid the influence of instabilities of the solution as well as of the fluorimeter, the full transition curve was measured every day. Since at both low and high concentrations of GdnHCl the equilibrium value of the fluorescence was reached within 16 h, these values could be used as internal reference values for native and completely unfolded protein throughout the remaining time. Each point of the GdnHCl induced transition curve at each day represents the average of 4 readings. These experiments permitted us to determine accurately the very small unfolding rate constants at 4.4, 4.5, and 4.6 M GdnHCl. It is well-known that Tyr fluorescence itself is a function of GdnHCl concentration (*31*). This was taken into account by measuring at the various GdnHCl concentrations the fluorescence of a Tyr solution with the same molarity as that of Tyr in the protein solution. The correction was only significant for solutions containing the completely unfolded protein, that is, at high GdnHCl concentrations (>4 M).

The unfolding kinetics of RM6 in 5.5−6.5 M GdnHCl were studied by injecting manually the protein solution with a Hamilton syringe into the respective GdnHCl solutions and measuring after proper stirring the fluorescence with a dead time of about 20 s. The excitation wavelength was 275.5 nm, the increment time 0.5 s, the slit width 1 mm, and the emission wavelength 303 nm.

Circular Dichroism Measurements. The sodium phosphate buffer, GdnHCl, and the protein solutions were mixed in a cuvette of 1 cm path length (Hellma) to obtain protein concentrations in the range 0.05−0.125 mg/mL. The ellipticity at 222 nm was measured as a function of time using a CD 6-dichrograph (Jobin-Yvon). At this wavelength the CD signals were linear in concentration. The operational low and high limits of high voltage of the CD6-Dichrograph are 275 and 750 V, respectively. In all measurements we kept high voltage between 300 and 500 V. Due to mixing of the solutions and the delayed automatic start of the CD run, the dead time was about 20 s. Calibration of the instrument was made using an epi-androsteron solution in dioxan of 1.25 mg/mL. A value of $\Delta A = 1.4 \times 10^{-3}$ at 304 nm (1 cm cuvette) was used as reference value.

Data Analysis

The kinetic constants and the activation energies have been derived using the following equations for the hypothetical unfolding mechanism illustrated in eq 1.

$$N_4 \xrightarrow{\text{fast}} 2N_2 \xrightarrow{\text{slow}} 4U \tag{1}$$

As will be pointed out later, we can assume that the observed CD and fluorescence changes reflect only the second part of the reaction sequence given by

$$N_2 \xrightarrow{\text{slow}} 2U.$$

We analyzed the unfolding reaction in terms of both first- and second-order mechanisms. The time course of ellipticity of a first-order unfolding process is described by the equation

$$\Theta - \Theta_\infty = (\Theta_0 - \Theta_\infty)e^{-k_1 t} \tag{2}$$

Second-order unfolding of RM6 was analyzed using eq 3.

$$\Theta = \Theta_\infty + \left(\frac{(\Theta_0 - \Theta_\infty)}{1 + k_2[N_2]_0 t}\right) \tag{3}$$

Θ_0 is the ellipticity at 222 nm of the dimeric nativelike intermediate, whose ellipticity cannot be discriminated from the ellipticity of the tetrameric RM6. The value is $\Theta_0 = -32\,000$ $deg \cdot cm^2 \cdot dmol^{-1}$. In the fits this parameter has been kept constant. Θ_∞ is the ellipticity of the unfolded monomer at $t \rightarrow \infty$ s.

Determination of Activation Parameters. The effect of temperature on the rate of unfolding of RM6 was analyzed according to the transition-state theory (*32*) using the Eyring equation in the form

$$\ln\frac{hk}{k_B T} = -\frac{\Delta H^\#}{RT} + \frac{\Delta S^\#}{R} \tag{4}$$

where k_B is Boltzmann's constant, h Planck's constant, and R the gas constant. $\Delta H^\#$ and $\Delta S^\#$ are the changes in standard enthalpy and entropy of activation. The relationship between the frequently determined Arrhenius activation energy E_A

(*33*), and the activation enthalpy $\Delta H^{\#}$ is given by eq 5.

$$\Delta H^{\#} = E_A - RT \tag{5}$$

Thus near room temperature E_A will be roughly 2.5 kJ·mol^{-1} larger than $\Delta H^{\#}$.

Determination of the Order of the Reaction. To derive the order of the reaction, the initial unfolding velocity was measured using different protein concentrations. On the basis of eq 6 the order with regard to concentration, *n*, was

$$\ln \upsilon_0 = \ln k + n \ln c_0^{\text{dimer}} \tag{6}$$

obtained from the slope of a plot of the logarithm of the initial velocity, υ_0, versus the logarithm of the initial dimer concentration, c_0^{dimer}.

Calculation of the Standard Gibbs Energy of Unfolding ΔG_D°. The equilibrium constant, *K*, of a tetramer-to-monomer equilibrium $N_4 \rightleftharpoons 4U$ is given by the equation

$$K = \frac{[U]^4}{[N_4]} \tag{7}$$

Defining the degree of unfolding, α, by the ratio $[U]/C_0$ of unfolded monomers and the total protein concentration in terms of monomers, C_0, the relation between *K* and the total monomer concentration can be expressed by the equation

$$K = \frac{4\alpha^4 C_0^{\,3}}{(1-\alpha)} \tag{8}$$

The standard Gibbs energy change is then given by the relation

$$\Delta G_D^0 = -RT \ln K \tag{9}$$

If unfolding is induced by GdnHCl at different concentrations of the denaturant, an apparent standard Gibbs energy change, $\Delta G_{D,app}^0$, is obtained experimentally that is a function of the denaturant concentration. Frequently it is a valid approximation to assume that the relationship between $\Delta G_{D,app}^0$ and the GdnHCl concentration is linear (*34*, *35*) as shown in eq 10.

$$\Delta G_{D,app}^0 = \Delta G_D^0 - m[\text{GdnHCl}] \tag{10}$$

The standard Gibbs energy change in the absence of the denaturant is obtained as the *y*-axis intercept in the plot of $\Delta G_{D,app}^0$ versus [GdnHCl]. *m* is the slope of the line.

Construction of Standardized Transition Curves. To standardize the fluorescence transition curves, the degree of unfolding, α, is expressed in the following manner

$$\alpha = \frac{[U]}{C_0} = \frac{y - y_0}{y_\infty - y_0} \tag{11}$$

The *y* values are the fluorescence values at a given GdnHCl concentration at time *t* and temperature *T*. y_0 and y_∞ are the fluorescence intensities of the native and unfolded protein

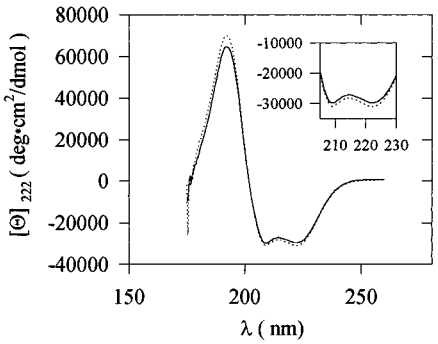

FIGURE 1: CD spectra of RM6 in 10 mM sodium phosphate, 10 mM Na_2SO_4, and 1 mM EDTA, pH 7.0, 25 °C: protein concentration, 1 mg/mL; solid line, spectrum after 900 h; dotted line, spectrum after 16 h. The insert provides an enlarged view.

($t \rightarrow \infty$ s), respectively. At high GdnHCl concentration (6.5 M), complete unfolding is observed after 16 h.

RESULTS

Stability of RM6. Figure 1 shows the CD spectra of a 1 mg/mL (76.7 μM of dimer) RM6 solution at 25 °C and pH 7.0 (10 mM sodium phosphate, 10 mM Na_2SO_4, 1 mM EDTA) immediately after dialysis to equilibrium with buffer (16 h; dotted line) and after standing for 900 h in a closed Eppendorf cup (solid line). The close identity of the two CD spectra indicates that the secondary structure of RM6 is practically not affected by standing for over a month. After 900 h the mean residue ellipticity based on $\bar{M} = 114.4$ [g/residue] is still −31 200 deg·cm^2·dmol^{-1} which is identical within error limits to the value of native RM6 which is $[\Theta]_{222}$ = −32 000 deg·cm^2·dmol^{-1}.

It is obvious that in principle the identity of the CD curves permits only the conclusion that the secondary structure is unaltered. To prove that also the tertiary fold of the tetrameric α-helix structure of RM6 has been maintained, DSC measurements have been performed with a fresh solution as well as with a solution that has been standing for 900 h. The heat capacity curves were found identical (not shown).

This result is excellent support for the intact nature of the protein even after exposure to such long-term storage in solution. On the basis of this finding, unfolding reactions could be monitored with confidence over the period of 900 h required for the establishment of equilibrium at 19 °C at intermediate GdnHCl concentrations.

RM6 Unfolds in a Second-Order Reaction. The manner in which the rate of a reaction varies with concentration can often be indicated by stating the order of the reaction. Two distinct orders of a reaction can be defined (*36*), one being the order with respect to concentration which relates the rate to concentration, the other being the order with respect to time, which is the order that is obtained using the method of integration of the rate equation. Since it is only at the beginning of the reaction that the conditions are known with certainty, it is evident that the order with respect to concentration is the more fundamental quantity. When both orders are identical, it can be inferred that no reaction products interfere with the reaction. For RM6 unfolding this would mean that denatured protein monomers do not affect the mechanism of tetramer disintegration.

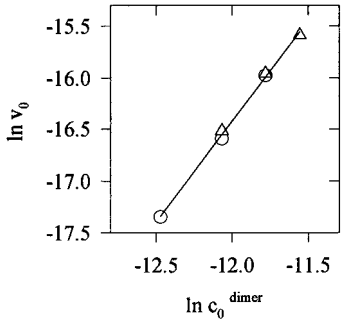

FIGURE 2: Concentration dependence of the initial unfolding velocity v_0 of RM6 after injection of the protein solution into 6.5 M GdnHCl in 10 mM sodium phosphate, 10 mM Na_2SO_4, and 1 mM EDTA, pH 7.0, 25 °C: logarithm of the initial velocity, ln v_0, plotted against the logarithm of the initial protein concentration; circles and triangles refer to independent experiments involving different protein preparations; protein concentrations were 0.05, 0.075, 0.1, and 0.125 mg/mL. The CD signal is linearly dependent on concentration in this concentration range.

Figure 2 illustrates the dependence on concentration of the initial unfolding velocity of RM6 observed after injection into 6.5 M GdnHCl solution at pH 7 and 25 °C. The logarithm of the initial velocity, ln v_0, has been plotted against the logarithm of the initial protein concentration, ln c_0^{dimer}. The slope of the linear graph gives the order of the reaction with respect to concentration. A value of 1.95 has been observed which strongly suggests that RM6 unfolds in a second-order reaction.

Order with Respect to Time. A series of representative, CD-monitored (222 nm), kinetic unfolding traces at 25 °C is shown in Figure 3 for various protein concentrations. Given also are the simulated curves based on first order (dotted traces) and second-order fits (solid lines). Unfolding was initiated by injection of the protein solution into 6.5 M GdnHCl. The measurements have been reproduced several times with protein from different preparations to exclude that artifacts were responsible for the extraordinary result of second-order unfolding.

The differences between experimental and calculated curves are given as residuals in millidegrees as a function of time for the second-order fit. It is evident that there is excellent agreement between theoretical and observed kinetic curves, if RM6 unfolding is assumed to proceed in a second-order reaction. Evidently, the agreement is very poor when a first-order process is used as basis for the fit, as a comparison between the dotted and solid curves shows. The initial unfolding velocities, second-order rate constants, and protein concentrations have been summarized in Table 1. It is seen that the average rate constant at 25 °C and 6.5 M GdnHCl is $\bar{k}_2 = 4200$ L·(mol of dimer)$^{-1}$·s^{-1}. The overall error has been estimated to be 6% which corresponds to ±250 L·(mol of dimer)$^{-1}$·s^{-1}.

Temperature Dependence of the Rate Constant of Unfolding. Analogous measurements have been performed at 7 different temperatures between 20 and 34 °C to obtain the temperature dependence of the rate constant. At all temperatures, the unfolding kinetics can be represented unambiguously by a second-order reaction. The values of the rate constants obtained from these curves have been summarized in Table 2.

A least-squares analysis of the data demonstrates that in the temperature range studied the activation enthalpy is independent of temperature. According to eq 4 the slope of the line provides a value for the activation enthalpy, $\Delta H^{\#}$, and the intercept with the ordinate gives a value for the entropy of activation, $\Delta S^{\#}$. The values obtained here are $\Delta H^{\#} = 29.1$ kJ·(mol of dimer)$^{-1}$ and $\Delta S^{\#} = -78.7$ J·(mol of dimer)$^{-1}$·K^{-1} and they refer to a GdnHCl concentration of 6.5 M (see Table 5).

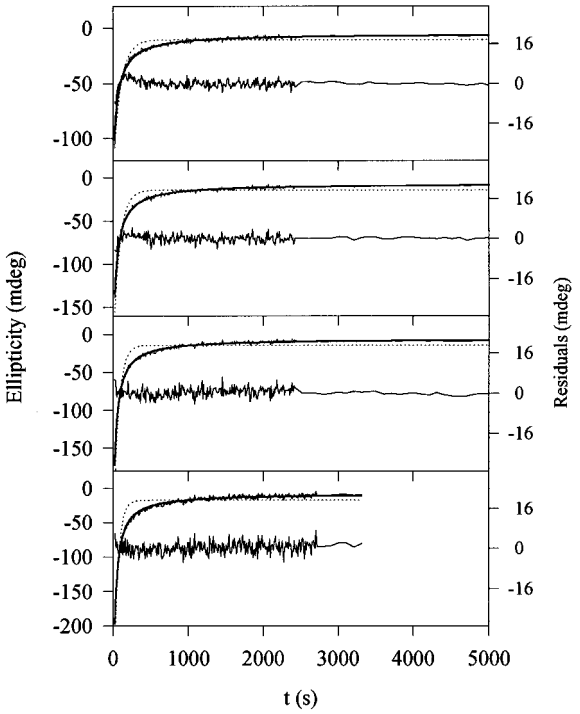

FIGURE 3: Unfolding of RM6 in 10 mM sodium phosphate, 10 mM Na_2SO_4, and 1 mM EDTA, pH 7, 25 °C; the reaction was initiated by a jump from 0 to 6.5 M GdnHCl and monitored by CD at 222 nm; protein concentrations from top to bottom were 0.05, 0.075, 0.1, and 0.125 mg/mL; solid line, second-order fit (eq 3); dashed line, first-order fit (eq 2); residuals, second-order fits. The graph shows only each 10th measured value; after 2500, measurements were made every second.

Table 1: Kinetic Parameters of RM6 Unfolding at 25 °C Derived from CD Measurements at 222 nm[a]

c_0, mg/mL (μM of dimer)	v_0,[b,c] mol/(L·s)	k_2,[c,d] L/(mol·s)
0.050 (3.84)	2.92×10^{-8}	4695
0.075 (5.75)	6.22×10^{-8}	4004
0.075 (5.75)	6.72×10^{-8}	4434
0.100 (7.65)	11.5×10^{-8}	3913
0.100 (7.65)	11.7×10^{-8}	4043
0.125 (9.60)	17.0×10^{-8}	4004

[a] Buffer: 10 mM sodium phophate, 10 mM Na_2SO_4, 1 mM EDTA, pH 7. The reaction was initiated by a jump from 0 to 6.5 M GdnHCl. [b] v_0: initial velocity. [c] k_2 and v_0 refer to the mole of dimer ($M = 13\,042$ g·mol^{-1}). [d] k_2: second-order rate constant obtained from nonlinear least-squares fitting of the data to eq 3. The estimated overall error including concentration errors, temperature deviations, etc. is ±6% of the numerical value of the kinetic constant.

Dependence of the Unfolding Rate Constant on GdnHCl Concentration. It has been shown in earlier studies on simpler monomeric proteins (*2*, *3*, *37*−*40*) that the observed rate constant varied with the final GdnHCl concentration. Therefore it was of great interest to find out whether a similar dependence existed also for the more complex unfolding reaction of the tetrameric RM6 protein. Figure 4 shows a series of fluorescence-monitored unfolding velocity curves

Table 2: Temperature Dependence of the Second-Order Rate Constant k_2 of RM6 Unfolding Derived from CD Measurements at 222 nm[a]

T (°C)	21	25	25	28	30	30	32	33	34
k_2[b] [L·(mol·s)$^{-1}$]	3030	3913	4043	4420	4458	4472	5210	5462	5449

[a] Buffer: 10 mM sodium phosphate, 10 mM Na_2SO_4, 1 mM EDTA, pH 7. The reaction was initiated by a jump from 0 to 6.5 M GdnHCl. Protein concentration: 0.1 mg/mL (7.6 μM of dimer). [b] k_2: second-order rate constant obtained from nonlinear least-squares fitting of the data to eq 3. The estimated overall error including concentration errors, temperature deviations, etc. is ±6% of the numerical value of the kinetic constant. k_2 refers to the mole of dimer (M = 13 042 g·mol^{-1}).

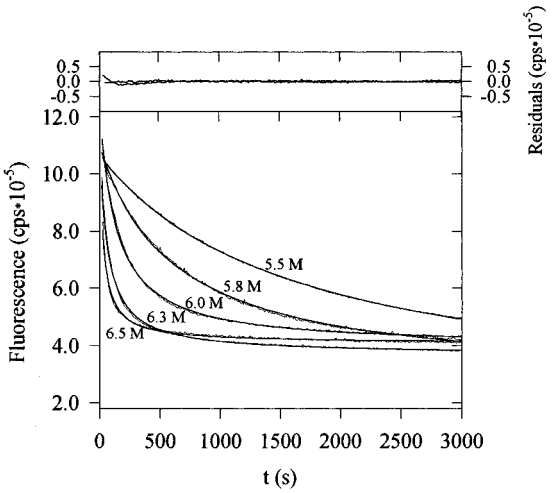

FIGURE 4: Fluorescence-monitored unfolding curves of RM6 in 10 mM sodium phosphate, 10 mM Na_2SO_4, and 1 mM EDTA, pH 7, 25 °C: protein concentration, 0.05 mg/mL; jump from 0 to 5.8, to 6.0, to 6.3, and to 6.5 M GdnHCl; solid lines, second-order fits according to eq 3; 1 cm cuvette; excitation wavelength, 275.5 nm; increment time, 0.5 s; slit, 1 mm; emission wavelength, 303 nm. Only every 10th measured value is shown; residuals are shown for the second-order fits for two experiments involving jumps from 0 to 6.3 M GdnHCl and from 0 to 5.8 M.

obtained at different final GdnHCl concentrations and the same RM6 concentration of 0.05 mg/mL (3.8 μM of dimer). The GdnHCl concentrations used were sufficiently high to fully unfold the protein.

It is evident from the curves that the unfolding rate increases dramatically with the increase in GdnHCl concentration. However, the mechanism of unfolding is the same for all GdnHCl concentrations. Each individual curve can again be fitted perfectly to the second-order equation over the full observation time. This can be seen from the random distribution of residuals around 0 which is given in the upper part of the graph. Since these unfolding reactions were monitored by fluorescence changes, which reflect tertiary structural changes rather than changes in α helicity seen in the CD studies, we can draw another significant conclusion. The second-order mechanism is observed in both CD and fluorescence studies, and a comparison of the magnitude of the rate constants shows clearly that they are identical within error limits. This result provides convincing evidence for the further conclusion that tertiary structural changes occur in synchrony with the changes in secondary structure. Therefore RM6 unfolding can be characterized as a highly cooperative process in agreement with the results obtained by our DSC studies (*1*). The second-order rate constants obtained from these decay curves have been summarized in Table 3.

To find out whether unfolding of RM6 secondary and tertiary structure is synchronized at all GdnHCl concentrations, this aspect has been studied in more detail in the following manner. Thirty-two sample vials were prepared containing different GdnHCl concentrations over the range 0−6.5 M at intervals of about 0.2 M. RM6 was injected to give a final concentration of 0.04 mg/mL (3 μM of dimer) in each vial, and 16 h after the injection, the first transition curve was monitored by fluorescence. A typical example is shown in Figure 5 a for a temperature of 30 °C.

On the basis of the kinetic traces shown in Figure 4, it can be inferred that, for the high GdnHCl concentrations (5.8−6.5 M), complete unfolding has occurred after 16 h. Therefore the fluorescence values which correspond to these high GdnHCl concentrations reflect the equilibrium situation. However, the fluorescence values of protein solutions containing lower GdnHCl concentrations are nonequilibrium data. To follow the approach to equilibrium the fluorescence of all 32 samples was measured at appropriate time intervals (1 or 2 days) and the resulting transition curves were constructed from these data. Some typical examples of such standardized, nonequilibrium transition curves are shown in Figure 5b. All data were obtained at 30 °C, and the time which had passed since the start of unfolding is given in the legend. The transition curve marked by open circles has been constructed from the original fluorescence data given in Figure 5a.

Similar time sequences of transition curves were also measured at 19, 25, and 35 °C. These experiments permitted us to determine accurately the very small unfolding rate constants at 4.4, 4.5, and 4.6 M GdnHCl as well as their variation with temperature.

Figure 6 illustrates the variation with temperature of the unfolding velocity of RM6. Typical degree of conversion versus time curves are shown which have been determined in 4.6 M GdnHCl at 35, 30, 25, and 19 °C, respectively. The solid lines have been calculated with the assumption of a second-order process using the equation $\alpha = \alpha_\infty - [\alpha_\infty/(1 + k_2[A_2]_0 t)]$ which is analogous to eq 3. α_∞ has been treated as an adjustable parameter whose value was found always equal to 1.0 ± 5%. It is evident that the second-order mechanism fits the experimental results perfectly. Similar measurements have been made at 4.4 and 4.5 M GdnHCl, and the unfolding rate constants determined for these 4 temperatures and 3 GdnHCl concentrations have been summarized in Table 4.

A comparison of the rate constants reveals the strong influence which the denaturant concentration has on their magnitude. Table 3 shows that the unfolding rate constant increases by 4 orders of magnitude at T = 25 °C when the GdnHCl concentration is increased from 4.4 to 6.5 M. The influence of temperature on the rate constant of unfolding at a given denaturant concentration is reflected in the activation parameters. These parameters have been obtained from linear fits of the data to the Eyring equation (eq 4).

The trends of the activation properties are unusual. All three parameters $\Delta G^{\#}$, $\Delta H^{\#}$, and $\Delta S^{\#}$ decrease with increasing

Table 3: Variation with GdnHCl Concentration of the Second-Order Rate Constant k_2 of RM6 Unfolding at 25 °C Derived from Fluorescence Measurements[a]

GdnHCl (M)	4.4[b]	4.5[b]	4.6[b]	5.5[c]	5.8[c]	6.0[c]	6.3[c]	6.5[c]
k_2[d] [L·(mol·s)$^{-1}$]	0.9	1.2	1.6	160	436	1766	3860	4304

[a] Buffer: 10 mM sodium phosphate, 10 mM Na_2SO_4, 1 mM EDTA, pH 7.0. [b] Protein concentration: 0.04 mg/mL (3.0 μM of dimer). [c] Protein concentration: 0.05 mg/mL (3.8 μM of dimer). [d] k_2: second-order rate constant obtained from nonlinear least-squares fitting of the data to eq 3. The estimated overall error including concentration errors, temperature deviations, etc. is ±6% of the numerical value of the kinetic constant. k_2 refers to the mole of dimer (M = 13 042 g·mol^{-1}).

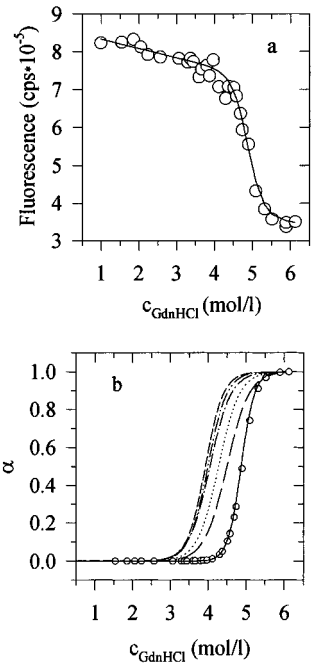

FIGURE 5: (a) Typical fluorescence-monitored GdnHCl induced nonequilibrium unfolding transition curve of RM6 obtained at 30 °C after 24 h of unfolding time: buffer, 10 mM sodium phosphate, 10 mM Na_2SO_4, and 1 mM EDTA, pH 7; protein concentration, 0.04 mg/mL; 1 cm cuvette; excitation wavelength, 275.5 nm; increment time, 0.5 s; slit, 1 mm; emission wavelength, 303 nm. (b) Approach to equilibrium demonstrated by normalized transition curves of RM6 determined in 10 mM sodium phosphate, 10 mM Na_2SO_4, and 1 mM EDTA, pH 7 at 30 °C: protein concentration, 0.04 mg/mL; 1 cm cuvette; excitation wavelength, 275.5 nm; increment, 0.5 s; slit, 1 mm; emission wavelength, 303 nm. The curves shown have been determined after the unfolding times indicated below: 16 h (—); 64 h (− − −); 112 h (···); 184 h (-·-·); 232 h (-···-··); 280 h (- - -). Circles: the same data as in part a after standardization of the transition curve. A comparison of the original and the normalized transition curves demonstrates the importance of reporting both typical experimental curves and normalized transition curves. Only if examples of both graphs are given can the possible influence of baseline extrapolations on the shape of the normalized curve be appreciated.

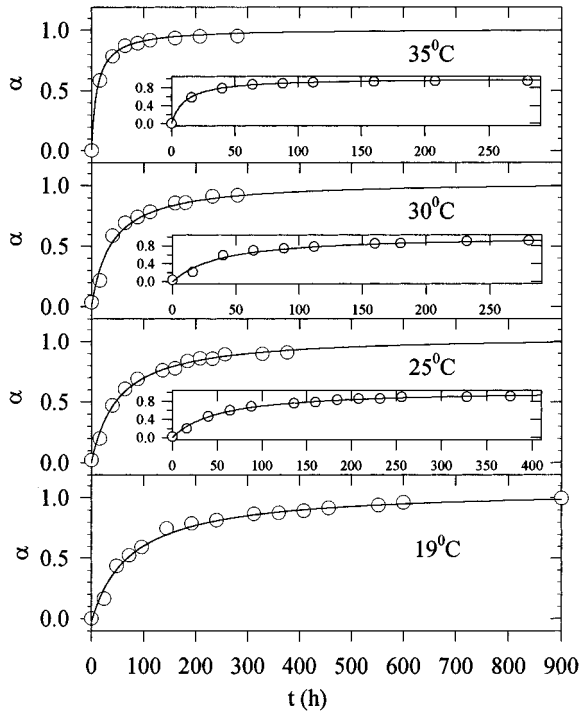

FIGURE 6: Variation with temperature of unfolding kinetics of RM6 at 4.6 M GdnHCl monitored by fluorescence. The graphs show the degree of conversion α (eq 11) of RM6 as a function of time and temperature in 10 mM sodium phosphate, 10 mM Na_2SO_4, and 1 mM EDTA, pH 7: protein concentration, 0.04 mg/mL; full line, second-order fit (eq 3); 1 cm cuvette; excitation wavelength, 275.5 nm; increment time, 0.5 s; slit width, 1 mm; emission wavelength, 303 nm; temperatures from top to bottom, 35, 30, 25, 19 °C. The inserts provide an enlarged view to demonstrate the quality of the fit.

Table 4: Temperature Dependence of the Second-Order Rate Constant k_2 of RM6 Unfolding Derived from Fluorescence Measurements[a]

	k_2[b] [L·(mol·s)$^{-1}$]		
T (°C)	4.4 M GdnHCl	4.5 M GdnHCl	4.6 M GdnHCl
19	0.5	0.7	1.2
25	0.9	1.2	1.6
30	1.5	2.0	2.5
35	2.7	3.1	4.5

[a] Buffer: 10 mM sodium phosphate, 10 mM Na_2SO_4, 1 mM EDTA, pH 7. Protein concentration: 0.04 mg/mL (3 μM of dimer). [b] k_2: second-order rate constant obtained from nonlinear least-squares fitting of the data to eq 3. The estimated overall error including concentration errors, temperature deviations, etc. is ±6% of the numerical value of the kinetic constant. k_2 refers to the mole of dimer (M = 13 042 g·mol^{-1}).

GdnHCl concentration. However, only $\Delta G^{\#}$ varies linearly while the activation enthalpy and entropy exhibit strongly nonlinear variations. It is worth noting that the activation entropy passes through 0 and turns negative between 4.4 and 4.5 M GdnHCl concentration. The change in sign of $\Delta S^{\#}$ compensates for the decrease in $\Delta H^{\#}$ thereby rendering the free energy of activation less sensitive to the increase in the denaturant concentration. The numerical values of the activation parameters have been summarized in Table 5.

DISCUSSION

The most prominent finding of the present study on a loop deletion mutant of ROP protein (RM6) is the fact that unfolding of the homotetramer proceeds as a second-order process. This is particularly intriguing, since so far all unfolding reactions of proteins have been reported to follow strictly a first-order mechanism except for the one example

Table 5: Activation Parameters of RM6 Unfolding at 25 °C[a]

[GdnHCl] (M)	4.4	4.5	4.6	6.5
$\Delta H^{\#}$ (kJ·mol^{-1})	79.7	67.5	60.7	29.1
$\Delta S^{\#}$ (J·mol^{-1}·K^{-1})	21.6	−16.7	−36.5	−78.7
$\Delta G^{\#}$ (kJ·mol^{-1})	73.3	72.5	71.6	52.6

[a] The Eyring parameters have been determined using eq 4 and refer to the mole of dimer (M = 13 042 g·mol^{-1}).

referred to later (*41*). Although the unfolding reaction has not yet been studied by stopped flow techniques, it can be concluded on the basis of an extrapolation of the ellipticity to time 0 that the second order determines the disappearance of RM6 structure from the very beginning. The extrapolated mean residue ellipticity at $t = 0$ is −32 000 deg·cm^2·dmol^{-1} ± 6% of RM6. This value of Θ_0 has been used in all fits to determine k_2 according to eq 3.

Given the notion that the order of a reaction does not permit the delineation of the molecularity whereas the opposite is well possible, it is not easy to rationalize the second order in molecular terms. A possible mechanism could be, however, the following. We assume that on exposure to GdnHCl the native RM6 tetramer dissociates fast into two dimers, with practically unchanged structure relative to that in the tetramer. Therefore neither the CD nor the fluorescence signals are detectably affected. In a second, rate-determining step, the dimers are thought to interact in such a manner as to initiate complete unfolding. This hypothetical unfolding mechanism has been illustrated in eq 1. Formally this mechanism could explain the second order, if the observed CD and fluorescence changes reflect only the second part of the reaction sequence given by

$$N_2 \xrightarrow{\text{slow}} 2U$$

We are aware that this mechanism is unusual for protein unfolding, since it implies interactions of two dimers in the activation step. However, it is completely consistent with the experimental observations at all temperatures and at all GdnHCl concentrations studied. Supportive evidence for the correctness of the model comes from the refolding reaction (Lassalle and Hinz, paper in preparation). To our knowledge there has been one report in the literature that describes higher orders than one being involved in the denaturation of an enzyme. That is the study by Casey and Laidler 1950 (*41*) on the irreversible heat inactivation of pepsin. The reaction rate was found to vary from fifth order in dilute solutions to first order in concentrated solutions, and simultaneously the activation energy decreased from 628 to 251 kJ·mol^{-1}. It is rather likely that in the case of pepsin the higher order rate law reflects aggregation or coagulation phenomena, whereas RM6 unfolding both by temperature and by GdnHCl is clearly unaffected by aggregation in the unfolded state (*1*). Therefore the finding of a second-order rate law for unfolding of proteins is unique so far. For small molecules in the gas phase, second-order decomposition is of course not unusual, as for example the well-characterized decomposition of hydrogen iodide demonstrates (*42*−*44*).

Comparison of Activation Parameters. Reaction rates almost always increase with temperature and in that regard RM6 unfolding provides no exception. However, variation with temperature of the unfolding rate of a protein can only be compared meaningfully with the unfolding rate of another protein, if comparable environmental conditions have been maintained for the two systems. In the present study on RM6 unfolding we employed as large as possible a variation in the denaturant (GdnHCl) concentrations to provide a wide enough platform for a reasonable comparison of the present results with literature data. The temperature dependence of the rate constant is commonly expressed in two ways. The first is the familiar Arrhenius equation; the second relation results from transition-state theory and is expressed by eq 4. Unfolding of RM6 appeared to be adequately characterized by temperature invariant activation parameters. Linear Arrhenius or Eyring plots have been obtained for a variety of unfolding reactions of proteins. Pohl observed such plots for tyrpsin (*45*) as well as for chymotrypsinogen (*46*). Segawa et al. (*47*, *48*) reported a linear plot for hen egg white lysozyme, Munson et al. (*20*) for the pseudo ROP wild type, and Ogasahara et al. (*49*) for the α subunit of tryptophan synthase. Furthermore, the cis−trans isomerization of proline as the rate-determining step in a considerable number of protein unfolding reactions exhibits a linear dependence on temperature (*50*). Curved Arrhenius plots for the unfolding reaction that would be indicative of a temperature-dependent activation enthalpy have been observed less frequently. One very thorough study in which curved Arrhenius plots have been found is that of Chen et al. (*38*) on T4 lysozyme. Therefore it is difficult to make generalizations due to the limited number of data available. The present results on RM6 support the conclusion that the change in heat capacity of activation for the passage from the folded to the transition state appears to be small or close to 0. The barrier for unfolding depends strongly also on entropic contributions. This becomes evident on inspection of the activation entropy changes summarized in Table 5 for 25 °C. With increasing GdnHCl concentration $\Delta S^{\#}$ passes through 0 and turns negative at the higher denaturant concentrations. Therefore with increasing GdnHCl concentrations the activation entropy changes in such a fashion as to actually increase the height of the barrier to unfolding by the positive ($-T\Delta S^{\#}$) contribution and thereby counteracts the decrease in $\Delta H^{\#}$. The only analogous finding has been reported by Chen et al. (*38*) for monomeric T4 lysozyme unfolding. The coupled decrease in activation enthalpy and entropy reflects an extraordinary feature uncommon to the majority of processes related to the stability of proteins. Most of these processes had been found to be compensatory in nature with enthalpies and entropies being of the same sign so that the two components of the free energy of activation, $\Delta H^{\#}$ and $-T\Delta S^{\#}$, tend to cancel. What this means in terms of interactions and mechanism remains to be established. Some new aspects of denaturant action have been observed, however, in our recent study on dielectric relaxation of ribonuclease A in the presence and absence of urea (*51*). Quantitative analysis of the relaxation spectra gave strong support to the idea that urea acts preferentially by perturbation of the water structure or more specifically by changing the dynamics of water. It appears as if the reduction in the percentage of associated solvent is instrumental in promoting unfolding. Although caution has to be exercised in uncritically transferring these findings on urea solutions to GdnHCl solutions in view of the differences in structure and charge of the two denaturants, qualitative similarities in their mode of action can be expected. The findings on urea would

support a mechanism of denaturant action that favors denaturant influence on the activity of water rather than suggesting direct binding interactions with the protein.

REFERENCES

1. Lassalle, M. W., Hinz, H.-J., Wenzel, H., Vlassi, M., Kokkinidis, M., and Cesareni, G. (1998) *J. Mol. Biol.* (in press).
2. Ogasahara, K., and Yutani, K. (1994) *J. Mol. Biol. 236*, 1227−40.
3. Ogasahara, K., Matsushita, E., and Yutani, K. (1993) *J. Mol. Biol. 234*, 1197−206.
4. Matthews, C. R. (1993) *Annu. Rev. Biochem. 62*, 653−83.
5. Miranker, A. D., and Dobson, Chr. M. (1996) *Curr. Opin. Struct. Biol. 6*, 31−42.
6. Dyson, H. J., and Wright, P. E. (1996) *Annu. Rev. Phys. Chem. 57*, 369−95.
7. Steer, B. A., and Merrill, A. R. (1997) *Biochemistry 36*, 3037−46.
8. Plaza del Pino, I. M., Parody Morreale, A., and Sanchez Ruiz, J. M. (1997) *Anal. Biochem. 244*, 239−55.
9. Laurents, D. V., and Baldwin, R. L. (1997) *Biochemistry 36*, 1496−504.
10. Lorimer, G. H. (1996) *FASEB J. 10*, 5−9.
11. Buchner, J. (1996) *FASEB J. 10*, 10−9.
12. Clarke, A. R. (1996) *Curr. Opin. Struct. Biol. 6*, 43−50.
13. Christians, E., Michel, E., and Renard, J. P. (1997) *Cell. Mol. Life Sci. 53*, 168−78.
14. Dill, K. A., and Chan, H. S. (1997) *Nat. Struct. Biol. 4*, 10−9.
15. Baldwin, R. L. (1994) *Nature 369*, 183−4.
16. Lazaridis, Th., and Karplus, M. (1997) *Science 278*, 1928−31.
17. Steif, Chr., Hinz, H.-J., and Cesareni, G. (1995) *Proteins: Struct., Funct., Genet. 23*, 83−96.
18. Steif, Chr., Hinz, H.-J., and Kokkinidis, M. (1994) *Struct. Biol. 10*, 706−16.
19. Steif, Chr., Weber, P., and Hinz, H.-J. (1993) *Biochemistry 32*, 3867−76.
20. Munson, M., Anderson, K. S., and Regan, L. (1997) *Folding Des. 2*, 77−87.
21. Peters, K., Hinz, H.-J., and Cesareni, G. (1997) *Biol. Chem. 378*, 1141−52.
22. Wells, J. A. (1996) *Proc. Natl. Acad. Sci. U.S.A. 93*, 1−6.
23. Clackson, T., and Wells, J. A. (1995) *Science 267*, 383−6.
24. Milla, M. E., and Sauer, R. T. (1994) *Biochemistry 33*, 1125−33.
25. Harbury, P. B., Kim, P. S., and Alber, T. (1994) *Nature 371*, 80−3.
26. Mann, C. J., Shao, X., and Matthews, C. R. (1995) *Biochemistry 34*, 14573−80.
27. Shao, X, Hensley, P., and Matthews, R. C. (1997) *Biochemistry 36*, 9941−9.
28. Nozaki, Y. (1972) *Methods Enzymol. 26*, 43−50.
29. Castagnoli, L., Scarpa, M., Banner, D. W., Tsernoglou, D., and Cesareni, G. (1989) *EMBO J. 8*, 621−9.
30. Perkins, S. J. (1986) *Eur. J. Biochem. 157*, 169−80.
31. Schmid, F. X. (1989) in *Protein structure a practical approach* (Creighton, T. E., Ed.) pp 255−7, IRL Press, New York.
32. Eyring, H. (1935) *Chem. Rev. 17*, 65−77.
33. Arrhenius, S. (1889) *Z. Phys. Chem. 4*, 226−48.
34. Bolen, D. W., and Santoro, M. M. (1988) *Biochemistry 27*, 8069−74.
35. Shirley, B. A. (1992) in *Stability of Protein Pharmaceuticals, Part A: Chemical and Physical Pathways of Protein Degradation* (Ahern, T. J., and Manning, M. C., Eds.) pp 167−194, Plenum Press, New York.
36. Lefort, M. (1937) *J. Chim. Phys. 34*, 206−12.
37. Creighton, T. E. (1994) *Struct. Biol. 1*, 135−8.
38. Chen, B.-Lu, Baase, W. A., and Schellmann, J. A. (1989) *Biochemistry 28*, 691−9.
39. Chen, B.-Lu., and Schellmann, J. A. (1989) *Biochemistry 28*, 685−91.
40. Chen, B.-Lu, Baase, W. A., Nicholson, H., and Schellmann. J. A. (1992) *Biochemistry 31*, 1464−76.
41. Casey, E. J., and Laidler, K. J. (1950) *Science 111*, 110−20.
42. Bodenstein, M. (1899) *Z. Phys. Chem. 29*, 295−314.
43. Kistiakowsky, G. B. (1928) *J. Am. Chem. Soc. 50*, 2315−30.
44. Lewis, W. C. McC. (1918) *J. Chem. Soc. 113*, 471−8.
45. Pohl, F. M. (1968) *Eur. J. Biochem. 7*, 146−52.
46. Pohl, F. M. (1976) *FEBS Lett. 65*, 293−6.
47. Segawa, Sh.-I., and Sugihara, M. (1984) *Biopolymers 23*, 2473−88.
48. Segawa, Sh.-I., and Sugihara, M. (1984) *Biopolymers 23*, 2489−98.
49. Ogasahara, K., and Yutani, K. (1997) *Biochemistry 36*, 932−40.
50. Odefey, Chr., Mayr, L. M., and Schmidt, F. X. (1995) *J. Mol. Biol. 245*, 69−78.
51. Abou-Aiad, T., Becker, U., Biedenkamp, R., Brengelmann, R., Elsebrock, R., Hinz, H.-J., and Stockhausen, M. (1997) *Ber. Bunsen-Ges. Phys. Chem. 101*, 1921−7.

BI9730691